



## Two-electron quantum dots as scalable qubits

T.P. Spiller, J.H. Jefferson<sup>1</sup>, M. Fearn<sup>1</sup>, D.L.J. Tipton<sup>1</sup>

Trusted E-Services Laboratory

HP Laboratories Bristol

HPL-2002-175 (R.1)

August 12<sup>th</sup>, 2002\*

E-mail: [jhjefferson@qinetiq.com](mailto:jhjefferson@qinetiq.com)

qubit,  
quantum  
computing,  
quantum dot

We show that two electrons confined in a square semiconductor quantum dot have two isolated low-lying energy eigenstates, which have the potential to form the basis of scalable computing elements (qubits). Initialisation, one-qubit and two-qubit universal gates, and readout are performed using electrostatic gates and magnetic fields. Two-qubit transformations are performed via the Coulomb interaction between electrons on adjacent dots. Choice of initial states and subsequent asymmetric tuning of the tunnelling energy parameters on adjacent dots control the effect of this interaction.

\* Internal Accession Date Only

Approved for External Publication

<sup>1</sup> QinetiQ, Sensors and Electronics Division, St. Andrews Road, Malvern, WR14 3PS, UK

© Copyright Hewlett-Packard Company 2002

# Two-electron quantum dots as scalable qubits

J.H. Jefferson,\* M. Fearn, and D.L.J. Tipton  
*QinetiQ, Sensors and Electronics Division,  
St Andrews Road, Malvern, WR14 3PS, UK*

T.P. Spiller  
*Hewlett-Packard Laboratories, Filton Road,  
Stoke Gifford, Bristol, BS34 8QZ, UK*

(Dated: July 30, 2002)

## Abstract

We show that two electrons confined in a square semiconductor quantum dot have two isolated low-lying energy eigenstates, which have the potential to form the basis of scalable computing elements (qubits). Initialisation, one-qubit and two-qubit universal gates, and readout are performed using electrostatic gates and magnetic fields. Two-qubit transformations are performed via the Coulomb interaction between electrons on adjacent dots. Choice of initial states and subsequent asymmetric tuning of the tunnelling energy parameters on adjacent dots control the effect of this interaction.

PACS numbers: 03.67.Lx, 68.65.+g, 73.23.Ad, 73.20.Dx, 71.45.Gm, 73.61.-r

---

\*Electronic address: [jhjefferson@qinetiq.com](mailto:jhjefferson@qinetiq.com)

## I. INTRODUCTION

Interest in quantum computing began to grow rapidly after the discovery of the factoring [1, 2] and searching [3] algorithms, which demonstrate that if a quantum computer could be built it would be capable of tasks impossible with conventional classical machines. This interest was further stimulated by the development of quantum error correction [4, 5] and fault tolerant [6, 7] techniques. These show that, rather than requiring the decoherence of the qubits comprising a quantum computer to be completely negligible during the evolution corresponding to a computation, it simply needs to be small. Then the redundant encoding of quantum information using additional quantum bits (and the more sophisticated fault-tolerant techniques) can be employed to maintain the coherence of the qubits effectively responsible for running the quantum algorithm. All this was a real stimulation for quantum computing hardware. Real quantum systems always have some level of decoherence and whilst it is hard to envisage removing this completely, making it small is a reasonable practical goal.

Consequently, over the past few years numerous systems have been examined (theoretically and/or experimentally) to assess their potential for qubits and quantum computing hardware [8]. These include photons [9], ions in an electromagnetic trap [10–13], atoms in beams interacting with cavities at optical [14] or microwave [15] frequencies, electronic [16] and spin [17] states in quantum dots, nuclear spins in a molecule in solution [18, 19] or in solid state [20], charge (single Cooper pair) states of nanometre-scale superconductors [21, 22], flux states of superconducting circuits [23–26], quantum Hall systems [27] and states of electrons on superfluid helium [28].

Five main criteria have been identified for quantum computing hardware [8, 29]: (i) Clearly identifiable qubits and the ability to *scale up* in qubit number; (ii) The ability to prepare “cold” initial states (such as the thermal ground state of the whole system); (iii) Small decoherence (so correction [4–6] can be utilized) - a rough benchmark is a fidelity loss of  $10^{-4}$  in an elementary quantum gate operation; (iv) The ability to realize a universal set of quantum gates – arbitrary single qubit rotations and an entangling two-qubit gate are enough to build up any general evolution [30–32]; (v) The ability to measure (in the usual sense of projective quantum measurements) qubits to determine the outcome of a computation.

Any qubit candidates have to be assessed against this “DiVincenzo checklist”, to see how they fare. Although all the above-mentioned candidates do reasonably well, there is to date no clear favourite route for quantum computing hardware. It is certainly true that so far the few-qubit experiments which have been performed have used fundamental entities for qubits, such as photons, atoms, ions or nuclear spins (in liquid state NMR). Such systems exist or can be placed in low-decoherence environments and have thus provided the first few-qubit demonstrations. However, it seems likely that *scalability* in qubit number, up to the size of useful many-qubit devices, may well be more easily achieved with condensed matter systems, making use of fabrication or self-assembly techniques to produce many-qubit arrays. The trade-off is that decoherence in such systems is generally higher than for fundamental qubits.

At present, there is thus considerable interest in solid state approaches to qubits. These have to match up well against (i), (ii), (iv) and (v) of DiVincenzo’s list, and in the first instance for (iii) must at least offer small enough decoherence for the demonstration of quantum gates. With flexibility in fabrication, choice of materials, etc., it is then possible that decoherence may be reduced down to the required level for actual quantum computation. In this paper we discuss a solid-state approach to qubits based on a particular form of quantum dot.

In some recent work [33, 34] we have shown that a few electrons in polygonal quantum dots, which are sufficiently large that the mean electron separation is greater than their effective Bohr radius, always have a charge-spin multiplet at low-energy which is well separated from higher-lying states. This isolation is a consequence of electron correlations, which tend to force the electrons into configurations close to their classical electrostatic ground state. Such states always have a quasi-degeneracy of at least  $2^N$  where  $N$  is the number of electrons, and further degeneracies may arise due to equivalent electrostatic minima [33]. An isolated ground multiplet of degeneracy  $m$  suggests that such systems could form the basis for a realisation of quantum computing elements, where each element is an  $m$  state quantum system or ‘qumit’. In this paper we focus on one such possibility, a square 2D semiconductor quantum dot containing two electrons. When the dot is large compared with the electron effective Bohr radius, the Coulomb repulsion dominates and tends to repel the electrons to diagonally opposite corners of the dot and the charge density is peaked in these regions, as shown in figure 1, in which the exact ground-state charge density is plotted. There are in fact 8 states in the ground manifold (2 singlets and 2 triplets) which arise from the two

base states shown in figure 2, each of which may be a singlet or a triplet depending on spin. These states could in principle form a base-8 quantum computing element. However, it is simpler to stay within one spin manifold, which is valid provided the spin-flip scattering time is sufficiently long. The initial state may be prepared in a given spin state in various ways. For example, in zero magnetic field at low temperatures the ground state is a singlet, whereas application of a magnetic field will give a triplet lowest when the flux through the dot is of order a half-integral number of flux quanta (see next section for further details). The Zeeman splitting will then give a spin-polarised ground state.

In the next section we analyse this system in detail and show how it forms the basis for a scalable qubit element. This element is very similar to the so-called quantum cellular automata, which has been proposed [35, 36] as a basic building block for a new kind of computing system in which the elements are either in one state (0) or the other (1). However, we emphasise that the system proposed here is fundamentally different in that we consider cellular automata as a fully coherent system in which the qubit (or array of qubits in general) are in superposition states in the true sense of quantum computation. Such quantum coherent cellular automata have been considered recently by Tóth and Lent [37] who also suggested square qubit cells consisting of four quantum dots in the corners. In this scheme there is vertical tunnelling between dots. Our work complements and extends theirs in several ways. Our qubit cells consist of a single quantum dot of square geometry in which the electrons are confined by their mutual Coulomb repulsion (strong correlation regime). The two-electron states are allowed to take on the full square symmetry with electrons tunnelling around the perimeter of the square. This lifts the spin degeneracy and produces independent two-state systems for singlets and triplets. These states are further controlled by corner gates and external magnetic fields. We also propose a new method of producing two-qubit entanglement via the Coulomb interaction .

## II. BASIC MODEL

We consider two electrons in a semiconductor quantum dot with a square confining potential in the  $x - y$  plane and sufficiently high confinement in the  $z$  direction that the electrons always occupy the lowest bound state in this direction. Such structures may be fabricated, for example, from a gated two-dimensional electron gas at a heterojunction in-

terface. In reality this would not produce a perfectly square confining potential though such deviations would not change qualitatively the results which follow and may be accounted for quantitatively by a straightforward extension of the theory. Further control of the two-electron states may be achieved by placing gate electrodes in the four corners of the dot, since applying a positive voltage to a corner electrode would provide a potential well for an electron in a region at the heterojunction interface below the gate. We consider low-lying two-electron states of the quantum dot in a magnetic field, which may be modelled using the 2D Schrödinger equation (after integrating over  $z$ ) [52]

$$i\hbar \frac{\partial \Psi(x, y, t)}{\partial t} = H \Psi(x, y, t) \quad (1)$$

where

$$H = \frac{1}{2m} \left[ \sum_{i=1}^2 (-i\hbar \nabla_i + e\mathbf{A}_i)^2 + V(\mathbf{r}_i, t) + E_B s_z^i \right] + \frac{e^2}{4\pi\epsilon|\mathbf{r}_1 - \mathbf{r}_2|} \quad (2)$$

and where  $V(\mathbf{r}, \mathbf{t})$  is the total one-electron confining potential,  $m$  is the effective mass of the electrons and  $\mathbf{A}$  is the vector potential of a magnetic field  $\mathbf{B}$  oriented perpendicular to the plane of the dot and  $E_B = g\mu_B B$  is the Zeeman energy. When the length-scale of the confining potential is small compared with the effective Bohr radius of the electrons, the eigenstates of  $H$  (with time-independent confining potential) may be computed to good accuracy using the Hartree-Fock approximation. This is rather like what is done in atomic physics and the term ‘artificial atoms’ has been used to describe such structures [38]. However, it should be realised that the energy scale is much smaller than in real atoms since the effective Bohr radius is typically two orders of magnitude larger. In this paper we shall be concerned with the opposite limit in which the size of the dot is large compared with the effective Bohr radius. In this regime, electron correlations become dominant since the Coulomb repulsion energy between the electrons scales like  $a/L$  whereas the electron kinetic energy scales like  $(a/L)^2$ , where  $a$  is the effective Bohr Radius and  $L$  is the confinement length. For large  $L/a$  the ground state of the electrons tend towards the classical minimum energy given by electrostatics. For the present case of two electrons in a square confinement potential, the electrons are pushed to diagonally opposite corners, as shown in figure 2. We can see immediately that such a ground state is degenerate since there are two equivalent positions which the pair of electrons may occupy and furthermore their spins may each take two values, giving a total degeneracy of 8 in the limit of infinitely large dots. For finite sized

dots with  $L/a \gg 1$ , kinetic energy partly lifts this degeneracy resulting in two singlets, with two degenerate triplets lying approximately midway between the singlets in zero magnetic field. This spectrum is shown in figure 3 for the case of a square quantum dot of side length  $800nm$  and material parameters corresponding to GaAs, giving a ratio  $L/a \approx 100$ . Also shown in the spectrum are the next few excited states, which are somewhat higher in energy. In fact this isolation of a low-lying multiplet is a common feature of few-electron states in the strongly correlated limit to which we refer to reference 33 for further details. This feature was also one of our main motivations for considering their use as quantum computing elements. However, one price to pay for this is that the absolute energy scale is small, though this is material dependent. For the given example, the singlet-separation in the ground manifold is of order  $5\mu eV$  whereas the next singlet is some  $33\mu eV$  higher in energy, as shown in figure 3. This spectrum was obtained numerically by expanding the eigenstates in basis functions of the noninteracting electron system and diagonalising the resulting Hamiltonian matrix. We emphasise that this seemingly simple problem requires considerable computing resources to obtain convergence for the lowlying eigenstates when the dot is large. For example, in the case of the  $800nm$  dot, the order of the matrices to be diagonalised was around 10000 and this grows rapidly with dot size. However, the simple electrostatic picture suggests that for the lowlying multiplet a simpler approximate method should be possible in which the electrons are in localised states near the corners of the dot. We have shown that this is the case in which one-electron Hartree states may be constructed, in which the electron is in one of the four corners. These are then used to construct suitable anti-symmetrised two-electron states, rather like Heitler-London molecular states. Restricting ourselves to the lowest Hartree states in the ‘ground manifold’ and eliminating higher energy states by quasi-degenerate perturbation theory gives excellent agreement with the numerically exact results and is computationally very efficient [39]. More importantly, it gives us a simple description of the lowest multiplet shown in figure 3, which may be described by the following effective Hamiltonian :

$$H_{\text{eff}} = \sum_{i=1}^4 \varepsilon_i(B)n_i + \left( \Delta(B)e^{i2\phi} R_{\pi/2} + \text{H.c.} \right) \quad (3)$$

where  $\varepsilon_i(B) = \varepsilon_i(0) + E_B s_z^i$ ,  $n_i = c_{i\uparrow}^\dagger c_{i\uparrow} + c_{i\downarrow}^\dagger c_{i\downarrow}$ ,  $R_{\pi/2}$  is a rotation operator which rotates both electrons simultaneously through an angle  $\pi/2$  about a point at the centre of the dot,  $\Delta(B)$  is an energy parameter which has only weak dependence on  $B$  (which we neglect)

and  $\phi$  is a Pierls phase factor which an electron picks up when hopping from a localised (Hartree) state on one corner to an adjacent corner. This phase factor is related to the total magnetic flux through the dot by  $4\phi = 2\pi\Phi/\Phi_0$ , where  $\Phi$  is the total flux through the dot and  $\Phi_0 = h/e$  is the flux quantum [53]. The zero field one-electron energies,  $\varepsilon_i(0)$ , depend on the corner gate voltages and may be used to force the ground-state of the system to be either one or the other of the states shown in figure 2. Conversely, when all 4 corner gate voltages are the same, the ground state is then an equal superposition of these base states. It is important to realise that  $H_{\text{eff}}$  only operates in the subspace defined by these base states, all other states consisting of electrons occupying adjacent corners of the dot must be omitted from the basis set. All such ‘excited’ base states (and many others corresponding to higher energy Hartree states) are accounted for in the energy parameters of equation (3). We stress that these parameters are calculated from the underlying Hartree states, not fitted to the numerically exact solutions. The method thus gives an efficient scheme for analysing the low-lying multiplet and calculating the associated energy parameters and their variation with magnetic field, dot geometry and gate potentials.

It is now straightforward to diagonalise  $H_{\text{eff}}$  within this restricted subspace for fixed magnetic field and gate potentials. If we neglect the Zeeman term, then the eigenstates must consist of two singlets and two triplets. These correspond to symmetric and anti-symmetric orbital states respectively. It is straightforward to show that the resulting  $2X2$  Hamiltonian matrices are:

$$H_{\text{singlet}} = \begin{bmatrix} E_0(B) & 2\Delta \cos(2\phi) \\ 2\Delta \cos(2\phi) & E_1(B) \end{bmatrix} \quad (4)$$

and

$$H_{\text{triplet}} = \begin{bmatrix} E_0(B) & 2\Delta \sin(2\phi) \\ 2\Delta \sin(2\phi) & E_1(B) \end{bmatrix} \quad (5)$$

where  $E_0(B) = \varepsilon_1(B) + \varepsilon_3(B)$  and  $E_1(B) = \varepsilon_2(B) + \varepsilon_4(B)$ , numbering clockwise from the top left-hand corner. The eigenenergies are thus,

$$E_{\text{singlets}} = \frac{E_0 + E_1 \pm \sqrt{(E_0 - E_1)^2 + 16\Delta^2 \cos^2 2\phi}}{2} \quad (6)$$

and

$$E_{\text{triplets}} = \frac{E_0 + E_1 \pm \sqrt{(E_0 - E_1)^2 + 16\Delta^2 \sin^2 2\phi}}{2} \quad (7)$$



These energies are in agreement with the exact low-lying multiplet shown in figure 3 for the special case when all corner gate voltages are the same ( $E_0 = E_1$ ) and zero magnetic field ( $\phi = 0$ ). At finite magnetic field, the energy of the singlets and triplets oscillate sinusoidally and also increase overall in energy with increasing magnetic flux through the dot, as shown in figure 4. The important points to note are that (i) the ground multiplet becomes a triplet with maximum splitting to the other triplet when half a flux quantum passes through the dot (and also for odd multiples of half a flux quantum) (ii) the coupling between states of the same symmetry may be ‘tuned’ by the magnetic field, e.g. when half a flux quantum passes through there is no coupling between singlets (degenerate) and maximum coupling between triplets [54]. These properties may be exploited for quantum computing in that the interstate coupling (and hence time scale) may be tuned. Furthermore, when the Zeeman term is switched on, the triplets split with the  $S_z = -1$  states lowest. Thus we may initialise the system to be in the lowest spin-polarised  $S_z = -1$  by choosing the magnetic field so that the magnetic flux through the dot is a half-integral, allowing the system to settle into its ground state at low temperature ( $T \ll E_B$ ). Alternatively, we may make a spin-singlet lowest in energy by choosing a magnetic field for which an integral number of flux quantum pass through the square, or indeed zero magnetic field. The choice of singlets or spin-polarised triplets for the qubit states is to some extent arbitrary but the choice should take into account the energy scales of the Zeeman splitting and the singlet-triplet splitting. For large dots,  $E_B$  can easily exceed  $\Delta$  and the spin-polarised state is preferred since all other states are pushed to higher energies. This has the disadvantage that the absolute energy/temperature scale is low, e.g. for an  $800\text{nm}$  square dot  $\Delta \approx 1\mu\text{eV} = 12\text{mK}$  in GaAs for which the Zeeman energy for a magnetic field of 1 tesla is about  $25\mu\text{eV} = 0.3\text{K}$ . Although such large dots have obvious advantages for fabrication and lithography, they would require very clean samples. Conversely, decreasing the dot size to, say,  $100\text{nm}$  raises  $\Delta$  to around  $0.5\text{meV} = 6\text{K}$  which is now somewhat greater than the 1 tesla Zeeman splitting. With corner gates this would be close to the present limits of what can be achieved by electron-beam lithography.

As with any 2-state system, we can map the Hamiltonian onto a pseudo-spin model, which takes the form,

$$H_{ps} = \bar{E} + \varepsilon\sigma_z + \gamma\sigma_x \quad (8)$$

where  $\sigma_x$  and  $\sigma_z$  are the usual Pauli operators,  $\bar{E} = (E_0 + E_1)/2$ ,  $\varepsilon = (E_1 - E_0)/2$ ,  $\gamma = 2\Delta \cos(2\phi)$  for singlets and  $\gamma = 2\Delta \sin(2\phi)$  for triplets. Despite the simplicity of this effective Hamiltonian, the main physics of the two-electron qubit system is contained within the energy parameters in equation (8), which have, in general, complicated functional dependencies on the confining region (defined by the boundary of the dot and gate electrode potentials), the mutual coulomb repulsion of electrons within the dot, and the external magnetic field through the dot. Nevertheless, these dependencies may be computed for any specific geometry and magnitudes of external potentials and fields and hence the parameters calibrated. In what follows we shall continue to refer to the 2-electron pseudo-spin base states as  $|0\rangle$  and  $|1\rangle$  to distinguish them from true single-electron spin base states  $|\uparrow\rangle$  and  $|\downarrow\rangle$ .

The Hamiltonian (2) and corresponding effective Hamiltonians (3) and (8) are readily generalised to two or more identical dots each containing two electrons. Such structures could be fabricated with gates and we envisage that the separation between the dots would be greater than the size of the dots themselves. This ensures that the Coulomb repulsion between electrons on different dots is always smaller than the Coulomb repulsion between the two electrons on the same dot and may thus be treated as a perturbation. Furthermore, the confining barriers and dot-dot separation ensures that tunnelling of electrons between dots, even as virtual states, is negligible. In this situation, only diagonal elements of the Coulomb interaction of the density-density type are non-negligible. Hence, the effective Hamiltonian for an array of  $N$  two-electron quantum dots may be written, in pseudo-spin notation (dropping a constant energy term):

$$H_{ps} = \sum_{i=1} [\varepsilon_i \sigma_{iz} + \gamma_i \sigma_{ix}] - \frac{1}{2} \sum_{i,j=1;i \neq j} v_{ij} \sigma_{iz} \sigma_{jz} \quad (9)$$

where the intra-dot energy parameters have the same meaning as in equation (8) and  $v_{ij}$  is half the difference in coulomb repulsion energy between dots  $i$  and  $i$  with parallel and anti-parallel pseudo-spins, i.e.

$$v_{ij} = \frac{\langle 0_i, 1_j | V_2 | 0_i, 1_j \rangle - \langle 0_i, 0_j | V_2 | 0_i, 0_j \rangle}{2} \quad (10)$$

where

$$V_2 = \frac{e^2}{4\pi\epsilon|\mathbf{r}_1 - \mathbf{r}_2|}. \quad (11)$$

Note that by symmetry,  $\langle 00|V_2|00\rangle = \langle 11|V_2|11\rangle$  and  $\langle 00|V_2|01\rangle = \langle 00|V_2|10\rangle = \langle 11|V_2|01\rangle = \langle 11|V_2|10\rangle$ .

If we neglect screening between electrons on different dots then since the electron wavefunctions are localised in the corner of the dots,

$$v_n \equiv v_{i,i+n} \simeq \frac{e^2}{8\pi\epsilon} \left( \frac{1}{nd-L} + \frac{2}{\sqrt{(nd)^2 + L^2}} + \frac{1}{nd+L} - \frac{2}{nd} - \frac{1}{\sqrt{(nd-L)^2 + L^2}} - \frac{1}{\sqrt{(nd+L)^2 + L^2}} \right) \quad (12)$$

where  $d$  is the spacing between adjacent dots. Expanding (1) in  $\frac{L}{nd}$  to lowest-order gives,

$$v_n \simeq \frac{3e^2}{4\pi\epsilon nd} \left( \frac{L}{nd} \right)^4$$

In practise, there will be some screening due to image charges in the corner gates giving,

$$v_n \simeq \frac{5e^2}{2\pi\epsilon} \left( \frac{\delta}{nd} \right)^2 \left( \frac{L}{nd} \right)^4$$

where  $\delta$  is the distance between an electron and its image charge. Hence,  $\frac{v_n}{v_1} = n^{-6}$  and while this decay is quite rapid, it is still sufficiently slow that the neglect of second and higher neighbour interactions would give rise to significant errors [40]. In section IV we show how such systematic errors may be reduced to acceptable levels by changing the tunnelling parameter  $\gamma$  on some of the dots. This effectively turns off the qubit interaction. In addition to restricting the effect of the Coulomb interaction to nearest neighbours, this technique is also used when performing single-qubit transformations for which even the nearest-neighbour coupling is turned off, as discussed elsewhere for qubits based on Josephson junctions [41, 42].

In the next two sections we will show how 2-electron square quantum dots described by this model and the pseudo-spin Hamiltonian (8), have potential for quantum computing elements.

### III. INITIALISATION AND SINGLE-QUBIT GATES

As emphasised by DiVincenzo and coworkers, a practical quantum computer has to satisfy a certain minimal list of requirements [29]. In this section we show how the 2-electron quantum dot can fulfil two of them, namely initialisation of the system and a universal single-qubit gate. Since the 2-electron quantum dot is an 8-state system, it is convenient to reduce

this to a 2-state ‘qubit’ system. This is not strictly necessary as in principle one can deal directly with octal elements though this poses many practical problems of implementation. The simplest way to reduce the quantum dot to a 2-state system is to essentially remove the spin degrees of freedom, as described in the previous section. This has the added advantage that the resulting two charge degrees of freedom may be manipulated electrostatically using gates. To be specific, we shall assume that we are dealing with singlets, for which the system is first allowed to relax into its ground-state at low-temperature and zero magnetic field (or constant field in which an integral number of flux quanta pass through the dot). The single cell may thus be described by only two coherent singlet states, with charge ordering as shown in figure 2 and effective Hamiltonian given by equation (4) or, equivalently, the pseudo-spin Hamiltonian, equation (8), with  $\gamma = 2\Delta \cos(2\phi)$ . We shall confine ourselves to this singlet manifold for the remainder of the paper, though it is straightforward to extend the results to the spin-polarised triplet states using the effective Hamiltonian given by equation (5). These states may be manipulated using the electrostatic gates in the four corners. For example, we may initialise the ‘0’ state by applying a large positive bias to corner gates 1 and 3 and allowing the system to relax to its ground state. Removing these potentials at  $t = 0$  will, according to equation (4) (with  $\cos 2\phi = 1$ ), cause the system to oscillate between the states  $|0\rangle$  and  $|1\rangle$  with a period  $T = \pi/2\Delta$ . This follows directly by expressing the initial state in terms of eigenvectors and applying the time evolution operator as follows.

$$\begin{aligned}
|\psi(t)\rangle &= e^{-iHt}|0\rangle = e^{-iHt} \frac{|+\rangle + |-\rangle}{\sqrt{2}} \\
&= \frac{e^{-iE_+t}|+\rangle + e^{-iE_-t}|-\rangle}{\sqrt{2}} \\
&= e^{-iE_0t} (\cos 2\Delta t |0\rangle + i \sin 2\Delta t |1\rangle)
\end{aligned} \tag{13}$$

where we have used

$$H = \begin{bmatrix} E_0 & 2\Delta \\ 2\Delta & E_0 \end{bmatrix} \tag{14}$$

giving  $E_{\pm} = E_0 \pm 2\Delta$  and  $|\pm\rangle = \frac{|0\rangle \pm |1\rangle}{\sqrt{2}}$ .

Thus, after time  $\pi/8\Delta$  a Hadamard transformation has taken place, with a NOT operation at time  $\pi/4\Delta$ . These timescales are typically of order a picosecond, e.g. for a 100nm dot in GaAs,  $T=0.6\text{ps}$ . The 2-state time translations given by equation (13) are not completely

general since they are restricted to a plane through the centre of the Bloch sphere [43]. However, the most general transformation, of the form:

$$|\psi(t)\rangle = e^{i\alpha(t)} \left[ \cos \theta(t)|0\rangle + e^{i\phi(t)} \sin \theta(t)|1\rangle \right] \quad (15)$$

may be achieved by applying a second rotation (time evolution) for which the Hamiltonian is changed by the application of a gate voltage to two diagonally opposite corners of the dot. This will change the energy of one of the base states in a predictable way. Neglecting the small change in the tunnelling matrix element  $\Delta$ , the new Hamiltonian takes the more general form of equation (4) with  $E_0 \neq E_1$ . When the energy difference between these diagonal matrix elements is much greater than  $\Delta$ , the eigenstates of the new Hamiltonian are approximately  $|0\rangle$  and  $|1\rangle$  and hence after a further time  $\tau$  we get,

$$\begin{aligned} |\psi(t + \tau)\rangle &= e^{-iHt}|0\rangle = e^{-it\tau} e^{-iE_0t} (\cos 2\Delta t|0\rangle + i \sin 2\Delta t|1\rangle) \\ &\approx e^{-iE_0(t+\tau)} (\cos 2\Delta t|0\rangle + i e^{-iE_g\tau} \sin 2\Delta t|1\rangle) \end{aligned} \quad (16)$$

where  $E_g = E_1 - E_0 \approx eV_g$ , and  $V_g$  is the gate potential. This clearly has the general form (15). It is straightforward to further generalise this procedure to any sequence of transformations in which gate voltages are changed in a stepwise fashion, *including* corrections to take into account the change in off-diagonal matrix elements of the Hamiltonian. In practise it may be advantageous to use a magnetic field to control the latter since they have little effect on the diagonal elements. For example, if we again apply a gate potential to the system in the state  $|\psi(t)\rangle$  given by equation (13), and simultaneously a magnetic field which produces half a flux quantum through the dot (thereby switching off the off diagonal matrix elements), we may again generate the general transformation (15), but with the advantage that the gate voltage need not be large. It may thus be ‘tuned’ to give the optimum switching time.

#### IV. TWO-QUBIT GATES

Two qubit transformations are performed using the coulomb interaction, i.e. the last term in the pseudo-spin Hamiltonian (9). A disadvantage of using the coulomb interaction for inter-qubit interactions is that it is difficult to control. DiVincenzo and coworkers circumvent this problem by modulating the exchange interaction between (real) spins on adjacent quantum dots by changing the potential barrier between them. In reference 37

three cells (qubits) were considered as a means of producing entanglement via the direct coulomb interaction. Here we consider a simpler scheme in which the effect of the coulomb interaction between two cells is controlled rather than its absolute value. The latter may only be changed by dynamical screening between cells, the possibility of which we consider briefly in the final section. In order for the coulomb interaction to be effective in producing entanglement between adjacent cells, we need to initialise the cells in such a way that a simple product state, degenerate or nearly so with some other product state, evolves into a linear combination of the two product states which cannot be factored in any basis. A potential candidate would be to start with one of the simple product states  $|0,0\rangle$ ,  $|0,1\rangle$ ,  $|1,0\rangle$  or  $|1,1\rangle$ , and observe the evolution. However, although this evolution does eventually produce full entanglement, it is dominated by single-qubit rotations (since  $\gamma \gg v$  in equation (9) with  $N = 2$ ), which produce rapid oscillations in the entanglement with time. We can in principle switch off these single-bit rotations with a magnetic field, for which  $\gamma = 0$  when a half-integral flux passes through the dot. However, this would also not lead to entanglement since the inter-dot Coulomb interaction is diagonal in the  $|0,1\rangle$  basis and the states initial state would remain a simple product. Indeed, we may choose such simple product states in the 'computational' basis as initial states prior to pure single qubit rotations in order to ensure that the states remain unentangled. Entanglement may be produced by initialising the two-qubit state as a simple product of *energy* eigenstates. These are obtained by diagonalising the single-qubit Hamiltonian, e.g. equation (8) with  $\varepsilon = 0$  and the constant energy term dropped, giving  $E_{\pm} = \pm\gamma$  and  $|\pm\rangle = (|0\rangle \pm |1\rangle)/\sqrt{2}$ . Starting in the product state  $|+, -\rangle$ , time evolution will mix in the state  $|-, +\rangle$  via the coulomb interaction, without which the state would not change. Note that *only* the  $|-, +\rangle$  state is mixed in since the Hamiltonian only couples to this state. This is analogous to the case of two electrons on the surface of liquid helium, for which the computational basis is given by the ground ( $|\alpha\rangle$ ) and first excited ( $|\beta\rangle$ ) states of each electron in a 1D Coulomb potential above the helium surface [28]. In this system, with no applied fields  $|\alpha, \beta\rangle$  and  $|\beta, \alpha\rangle$  are degenerate, but this degeneracy can be broken by a Stark shift on one of the qubits. The (weak) Coulomb interaction between adjacent qubits then splits the degeneracy, with eigenstates given by the symmetric and anti-symmetric superpositions of  $|\alpha, \beta\rangle$  and  $|\beta, \alpha\rangle$ . Starting with either  $|\alpha, \beta\rangle$  or  $|\beta, \alpha\rangle$  away from degeneracy (with the Stark shift dominating the coulomb splitting), and turning off the Stark shift for a chosen time, can in principle produce maximal entanglement

(a ROOT SWAP gate) with good fidelity [44]. In our quantum dot system, the state  $|-\rangle$  and  $|+\rangle$  play the role of  $|\alpha\rangle$  and  $|\beta\rangle$  in the helium system.

In the cell-diagonal energy basis, the two-qubit hamiltonian matrix is

$$\mathbf{H} = \begin{pmatrix} -2\gamma & 0 & 0 & -v \\ 0 & 0 & -v & 0 \\ 0 & -v & 0 & 0 \\ -v & 0 & 0 & 2\gamma \end{pmatrix} \quad (17)$$

where the rows and columns are ordered in ascending single-cell energy. The eigensolutions are shown in figure 5. It follows directly that the state vector at time  $t$  is

$$\begin{aligned} |\psi(t)\rangle &= e^{-iHt}|+, -\rangle = e^{-ivt}|g\rangle + e^{ivt}|e\rangle \\ &= \cos vt|+, -\rangle - i \sin vt|-, +\rangle \end{aligned} \quad (18)$$

which is clearly fully entangled for  $t = (2n + 1)\pi/4v, n = 0, 1, 2, \dots$ . The degree of entanglement is not so apparent in the original  $|0\rangle, |1\rangle$  basis. However, we may obtain an absolute measure of entanglement by computing the so-called concurrence [45] which is basis independent,

$$c(t) = 2|\langle a, a|\psi(t)\rangle\langle b, b|\psi(t)\rangle - \langle a, b|\psi(t)\rangle\langle b, a|\psi(t)\rangle| \quad (19)$$

where  $|a\rangle$  and  $|b\rangle$  are any orthonormal single-qubit basis states. Choosing these to be the energy eigenstates we see directly from (19) that

$$c(t) = |\sin 2vt| \quad (20)$$

showing that  $c(t) = 1$  again for  $t = (2n + 1)\pi/4v, n = 0, 1, 2, \dots$ . We note that the entanglement depends only on  $v$  and is independent of  $\gamma$ , the energy parameter which controls single-qubit rotations. By contrast, a plot of  $c(t)$  starting with a product state in the 'computational' basis, shows rapid oscillations on a timescale of  $h/\gamma$ , as shown in figure 6.

Two further issues arise when considering the above procedure for producing entangled states. The first is how to prepare the initial state,  $|+, -\rangle$ , and secondly how to preserve an entangled state once it has been produced, bearing in mind that the degree of entanglement oscillates with time. A further, and related, potential difficulty is being able to perform single-qubit operations for which the effect of the intra-cell coulomb interaction is made negligible. Clearly the most direct, and probably the most difficult, way to do this is by

selectively switching off the coulomb interaction between cells (see next section). An indirect way is to lift the degeneracy between the states  $|+, -\rangle$  and  $|-, +\rangle$  whilst the single qubit operations are being performed. For the Helium system it is proposed to implement this through application of an electric field to one electron creating a Stark shift [44]. For the quantum dots a magnetic field is applied to one dot but not the other, thereby changing the value of the tunnelling parameter  $\gamma$  on one of the dots. For example, if the magnetic flux through one of the dots is half a flux quantum the corresponding coupling is zero and the  $|+\rangle$  and  $|-\rangle$  states for that dot become degenerate. Hence the states  $|+, -\rangle$  and  $|-, +\rangle$  now differ in energy by  $2\gamma$ , where  $\gamma$  is the tunnelling parameter on the other dot. The eigensolutions of the two-cell Hamiltonian are then  $E = \pm\varepsilon$  and  $|g\rangle = \cos\theta|+, -\rangle + \sin\theta|-, +\rangle$  and  $|e\rangle = -\sin\theta|+, -\rangle + \cos\theta|-, +\rangle$ , where  $\varepsilon = \sqrt{\gamma^2 + v^2}$  and  $\tan\theta = \frac{v}{\gamma + \sqrt{\gamma^2 + v^2}}$ . If we again start in the state  $|+, -\rangle$  at  $t = 0$ , the state at time  $t$  becomes

$$|\psi(t)\rangle = e^{i\varepsilon t} \sin\theta|g\rangle + \cos\theta e^{-i\varepsilon t}|e\rangle = [e^{i\varepsilon t} \cos^2\theta + e^{-i\varepsilon t} \sin^2\theta] |+, -\rangle + i \sin 2\theta \sin \varepsilon t |-, +\rangle \quad (21)$$

Hence, the probability of finding the (other) state  $|-, +\rangle$  at time  $t$  is  $|\langle -, + | \psi(t) \rangle|^2 = \sin^2 2\theta \cos^2 \varepsilon t$  which has a maximum value of  $\sin^2 2\theta \approx (v/\gamma)^2$  when  $v/\gamma$  is small. This should be compared with the previous case for which the states and the maximum value of  $|\langle -, + | \psi(t) \rangle|^2$  is unity.

An alternative measure of the effectiveness of ‘detuning’ in preserving a state is the concurrence. This is zero for the state  $|+, -\rangle$  at  $t = 0$  and  $2|\sin 2\theta \sin \varepsilon t \sqrt{1 - \sin^2 2\theta \sin^2 \varepsilon t}|$  at later times when the system is in the state (21). This is plotted in figure 7 with  $\gamma = 0$  on the one dot and  $v/\gamma = 0.1, 0.2$  and  $1$  on the other. We see that the maximum concurrence decreases rapidly as the intra-dot tunnelling increases relative to the inter-dot coulomb interaction, with  $c_{max}(t) \approx 2 \sin 2\theta \approx 2v/\gamma = 0.2$  for  $v/\gamma = 0.1$ . Note also that when  $v/\gamma$  is small, the concurrence oscillates with angular frequency  $\varepsilon \approx \gamma$ . This should be compared with the case when  $\gamma$  is the same on both dots, for which  $c(t)$  oscillates between 0 and 1 at the much lower frequency  $2v$  (equation 20). We note that such detuning of the initial state in order to remove its degeneracy with the state  $|-, +\rangle$  may also be done by applying positive gate voltages to all four corner gates on one dot. This will change the confinement potential profile such as to again reduce the tunnelling parameter  $\gamma$ .

Although the above de-tuning procedure will significantly reduce the maximum concu-



rence caused by the Coulomb interaction, this may still give rise to systematic errors for single-qubit transformations that are not sufficiently small to be quantum error corrected. However, we have shown that the entangling effect of the Coulomb interaction may be eliminated completely by starting with product states that are diagonal in the 'computational' basis (i.e. the states  $|0,0\rangle$ ,  $|0,1\rangle$ ,  $|1,0\rangle$  or  $|1,1\rangle$ ) and setting  $\gamma = 0$  on one of the dots (or all dots apart from one in an array of qubits). Since the Coulomb interaction is diagonal in this basis, we might expect that it would be ineffective in producing entanglement since there are no single-qubit rotations on the dots for which  $\gamma = 0$ . This is indeed the case as may be proved by expressing the initial state in the basis of exact two-qubit eigenvectors, propagating with the time evolution operators, and re-expressing the result in product basis states, from which the concurrence is calculated and shown to be zero by exact cancellation. A related situation exists in the proposed scenario for Josephson junction qubits [41, 42], where it is not possible to do simultaneous one-qubit operations on adjacent qubits without turning on the (controllable) coupling between these qubits.

The concurrence may also be preserved by detuning a state that is maximally entangled. For example, we have shown that a fully entangled state may be produced at time  $t = \pi/4v$  (see equation 19). If at this time we change the Hamiltonian by switching off the tunnelling process in one dot (as described above), then the concurrence is,

$$\begin{aligned} c(t) &= |\sin 2vt| && (t \leq \pi/4v) \\ &= \sqrt{1 - \sin^2 2\theta \sin^2 2\varepsilon(t - \pi/4v)} && (t \geq \pi/4v) \end{aligned} \quad (22)$$

This is plotted in figure 8, again for  $v/\gamma = 0.1, 0.2$  and  $1$ , and we see that  $c(t)$  remains close to unity when  $v/\gamma$  is small. In fact, preservation of an entangled state is more effective than preservation of an unentangled state by this method (compare figure 7). Even the case  $\gamma = v$  has a minimum entanglement of  $c_{min} = 1/\sqrt{2} = 0.7071$  and rapidly approaches unity with decreasing  $v/\gamma$ . For small  $v/\gamma$  the correction  $\sim (v/\gamma)^2$  giving maximum deviations in concurrence of order a percent for realistic parameter values. Whilst this may still not be sufficiently small to allow full quantum error correction, it is well within the error necessary to unequivocally observe entanglement experimentally.

With the qubits essentially decoupled, we may prepare the initial state  $|+, -\rangle$  by single-qubit rotations. A novel way to do this is to first allow the two qubits to relax into their ground states, when a magnetic field is applied to one dot such that the magnetic flux

through the dot is one flux quantum. Removing this magnetic field at  $t = 0$  on the first dot will give the desired state since this exchanges the ground and excited states [39].

We have discussed here the realization of a ROOT SWAP gate, which is a suitable universal two-qubit gate [30–32]. It is well known how to convert such a gate into other two-qubit gates, such as a controlled phase flip or a CNOT, using single qubit rotations [46]. In any actual computation, the most suitable two-qubit gate(s) would depend upon the algorithm, also taking into account physical optimization [46]. For now, we remark that in the initial stages of investigation of new candidates for quantum computation, the most important two-qubit issue is the capability to produce entanglement. Thus the simplest gate to consider is that which requires no (or the minimum number of) additional single qubit gates. Experiments to investigate entanglement in dot systems such as those proposed here will therefore probably focus first on ROOT SWAP.

## V. SUMMARY AND DISCUSSION

In this paper we have analysed the potential of two electrons in square semiconductor quantum dots as a basis for a scalable array of quantum computing elements. As with all few-electron quantum dots in the strong correlation regime, there exists an isolated low-lying multiplet of states which has the potential to form a controllable finite-state system, or ‘qumit’. For two electrons, this is a two-state, i.e qubit, system for the orbital degrees of freedom. This requires that the spin-state (singlet or triplet) does not change during the computation period between initialisation and measurement. It has been argued elsewhere [47] that this is feasible due to the long lifetime of spin states in semiconductors, though it is by no means certain that these will be sufficiently long for practical implementation of a spin-based quantum computer. In addition to this, we require that the orbital states be sufficiently long-lived for meaningful computations to be made. This is also uncertain at present though various schemes can be envisaged which would reduce the inelastic scattering of electrons by the relevant acoustic phonons of energy equal to the energy splitting of the ground multiplet states. Note that at low-temperatures the main process would be spontaneous phonon emission and it had been suggested that this may be inhibited by device geometry and material choice at heterojunction interfaces [48]. Indeed, very recent theoretical work has demonstrated this quantitatively [49]. A further possibility would be

a molecular system for which the relevant low-lying electronic energy splitting would be chosen so that they were not resonant with the molecular vibrational modes. In order that the electrons remain strongly correlated in such a small molecular system, they would have to be screened by filled outer shells as in d or f electron systems [50].

Initialisation of our proposed system is performed by corner gates, which force each qubit into one of the two computational-basis states. Subsequent single-qubit operations (rotations) are then performed by removing the voltages on the corner gates and allowing the system to develop ballistically in time. Further control may be achieved during the computation phase by the application of a magnetic field, which changes the magnitude of the tunnelling energy parameter, and by further application of corner gate voltages. In this way we have shown that any single-qubit transformation may be performed.

We have shown how two-qubit transformations may be performed via the coulomb interaction between qubits provided this is small compared with the intra-qubit tunnelling energy. A potential problem is the control of the coulomb interaction itself. This is achieved by appropriate choice of initial states and intermediate states which are ‘tuned’ by changing the tunnelling parameter on one of the qubit-dots. In this way, entanglement is maximised via an initial state in which one dot is in its ground state and the other in its excited state. When this has been achieved, an entangled state is preserved by changing the tunnelling parameter in one dot only, via a magnetic field. A more direct control of the Coulomb interaction would be to physically change its magnitude during computation. This may be achieved in principle by introducing screening charge between the qubits. Control of this charge could be via surface gates or by controlling supercurrents, which are driven normal by exceeding their critical value. Although such schemes would be technologically challenging, they cannot be ruled out on fundamental grounds and may ultimately be a practical way forward in directly controlling the coulomb interaction.

Finally, we consider readout, i.e. the means of measuring the state after computation. For the spin system proposed by DiVincenzo and coworkers, a suggested method was to use spin-dependent tunnel barriers in which an electron of the appropriate spin would tunnel into a quantum confined region where it would be detected by a single-electron transistor [51]. A similar scheme is envisaged here but with the added simplicity that the tunnel barrier would not be spin dependent. It would be located at one or more corners of the quantum dot (one is sufficient in principle but more may be desirable to reduce errors). When the

qubit state is measured, the tunnel barrier is lowered and if an electron is in that corner of the dot it will tunnel into a quantum-confined region and be detected by the single-electron transistor. This uniquely defines the measured state. After measurement the system may be ‘reset’ using appropriate gate bias voltages.

Note that in order for a coherent time-development of the qubit to be negligible during the measurement process, the tunnel barrier must be lowered and raised on a timescale which exceeds the electron tunneling time but is sufficiently short for intra-dot time-development (e.g. single-qubit rotations) to be small, ideally negligible. This may be achieved in principle by the arrangement of gates shown schematically in figure 9. The square quantum dot (A) is extended at one corner by a quantum wire leading to a further quantum dot (B). This is essentially two very weakly coupled quantum dots for which the two electrons are normally located in the larger dot, A. As far as the quantum computation is concerned, the dots are decoupled and the states are controlled by corner gates as described earlier. The measurement is performed by lowering the electron potential energy in dot B via a positively biased gate (shown dotted). If an electron is in the corner of dot A, which is connected to dot B, then it will be transferred to the latter. Subsequently raising the electron potential energy of dot B to its ‘normal’ voltage will trap the electron in dot B where it can be later measured by a single-electron transistor. It should be realized that the process of transferring the electron from dot A to dot B does not necessarily destroy the coherence of the full quantum state involving both dots. If the initial single-qubit state is a superposition of states  $|0\rangle$  and  $|1\rangle$  then the final state after the possible transfer of an electron will also be a superposition of states in which an electron is either in dot B or not. However, since the two dots are essentially decoupled, this superposition does not change with time, unlike the ‘quantum computation’ states which continually oscillate between the base states. It is only when the presence (or not) of an electron on dot B is measured by the single-electron transistor that the wavefunction ‘collapses’ giving a probability that is essentially  $|\langle 0|\psi\rangle|^2$ .

### **Acknowledgments**

The authors would like to acknowledge helpful discussions with J. Annett, C. Creffield, B. Gyorffy, C. J. Lambert, I. A. Larkin, P. Meeson and W.J. Munro. This work was supported in part by the UK Ministry of Defence (corporate research programme).

- 
- [1] P. W. Shor, in *Proceedings of the 35th Annual Symposium on the Foundations of Computer Science*, edited by S. Goldwasser (1994), p. 124, quant-ph/9508027.
- [2] P. W. Shor, *SIAM J. Computing* **26**, 1484 (1997).
- [3] L. K. Grover, in *Proceedings of the 28th Annual ACM Symposium on the Theory of Computing (STOC)* (1996), p. 212, quant-ph/9605043.
- [4] P. W. Shor, *Phys. Rev. A* **52**, 2493 (1995).
- [5] A. M. Steane, *Phys. Rev. Lett.* **77**, 793 (1996).
- [6] A. M. Steane, *Phys. Rev. Lett.* **78**, 2252 (1997).
- [7] P. W. Shor, in *Proceedings of the 37th Symposium on the Foundations of Computer Science* (1996), p. 56, quant-ph/9605011.
- [8] A recent comprehensive (but by no means exhaustive) collection of papers can be found in *Fortschritte der Physik* **48**, Number 9-11, Special Focus Issue: Experimental Proposals for Quantum Computers, (2000).
- [9] E. Knill, R. Laflamme, and G. J. Milburn, *Nature* **409**, 46 (2001).
- [10] J. I. Cirac and P. Zoller, *Phys. Rev. Lett.* **74**, 4091 (1995).
- [11] J. I. Cirac and P. Zoller, *Nature* **404**, 579 (2000).
- [12] C. Monroe, D. M. Meekhof, B. E. King, W. M. Itano, and D. J. Wineland, *Phys. Rev. Lett.* **75**, 4714 (1995).
- [13] C. A. Sackett, D. Kielpinski, B. E. King, C. Langer, V. Meyer, C. J. Myatt, M. Rowe, Q. A. Turchette, W. M. Itano, D. J. Wineland, et al., *Nature* **404**, 256 (2000).
- [14] H. J. Kimble, M. Dagenais, and L. Mandel, *Phys. Rev. Lett.* **39**, 691 (1977).
- [15] S. Haroche, M. Brune, and J. M. Raimond, *Philos. Trans. Roy. Soc. London* **A355**, 2367 (1997).
- [16] A. Ekert and R. Jozsa, *Rev. Mod. Phys.* **68**, 733 (1996).
- [17] D. Loss and D. P. DiVincenzo, *Phys. Rev. A* **57**, 120 (1998).
- [18] N. A. Gershenfeld and I. L. Chuang, *Science* **275**, 350 (1997).
- [19] D. Cory, A. Fahmy, and T. Havel, *Proc. Nat. Acad. Sci. USA* **94**, 1634 (1997).
- [20] B. E. Kane, *Nature* **393**, 133 (1998).
- [21] A. Shnirman, G. Schön, and Z. Hermon, *Phys. Rev. Lett.* **79**, 2371 (1997).

- [22] Y. Nakamura, Yu. A. Pashkin, and J. S. Tsai, *Nature* **398**, 786 (1999).
- [23] M. F. Bocko, A. M. Herr, and M. J. Feldman, *IEEE Trans. Appl. Superconductivity* **7**, 3638 (1997).
- [24] J. E. Mooij, T. P. Orlando, L. Levitov, L. Tian, C. H. Van der Wal, and S. Lloyd, *Science* **285**, 1036 (1999).
- [25] J. R. Friedman, V. Patel, W. Chen, S. K. Tolpygo, and J. E. Lukens, *Nature* **406**, 43 (2000).
- [26] C. H. Van der Wal, A. C. J. ter Haar, F. K. Wilhelm, R. N. Schouten, C. J. P. M. Harmans, T. P. Orlando, S. Lloyd, and J. E. Mooij, *Science* **290**, 773 (2000).
- [27] V. Privman, I. D. Vagner, and G. Kventsel, *Phys. Lett. A* **239**, 141 (1998).
- [28] P. M. Platzman and M. I. Dykman, *Science* **284**, 1967 (1999).
- [29] D. P. DiVincenzo in *Mesoscopic Electron Transport*, (ed. L. Kowenhoven, G. Schön and L. Sohn), NATO ASI Series E, (Kluwer Ac. Publ., Dordrecht, 1997); cond-mat/9612126.
- [30] D. P. DiVincenzo, *Phys. Rev. A* **51**, 1015 (1995).
- [31] S. Lloyd, *Phys. Rev. Lett.* **75**, 346 (1995).
- [32] A. Barenco, C. H. Bennett, R. Cleve, D. P. DiVincenzo, N. Margolis, P. W. Shor, T. Sleator, J. Smolin, and H. Weinfurter, *Phys. Rev. A* **52**, 3457 (1995).
- [33] J. H. Jefferson and W. Häusler, *Molecular Physics Reports* **17**, 81 (1997).
- [34] C. E. Creffield, W. Häusler, J. H. Jefferson, and S. Sarkar, *Phys. Rev. B* **59**, 10719 (1999).
- [35] C. S. Lent, P. D. Tougaw, W. Porod, and G. H. Bernstein, *Nanotechnology* **4**, 49 (1993).
- [36] G. H. Bernstein, I. Amlani, A. O. Orlov, C. S. Lent, and G. L. Snider, *Nanotechnology* **10**, 166 (1999).
- [37] G. Tóth and C. S. Lent, *Phys. Rev. A* **63**, 052315 (2001).
- [38] M. A. Kastner, *Rev. Mod. Phys.* **64**, 849 (1992).
- [39] C. E. Creffield, J. H. Jefferson, S. Sarkar, and D. L. J. Tipton, *Phys. Rev. B* **62**, 7249 (2000).
- [40] We would like to acknowledge the referee for drawing our attention to this important point.
- [41] Yu. Makhlin, G. Schön, and A. Shnirman, *Nature* **398**, 305 (1999).
- [42] Yu. Makhlin, G. Schön, and A. Shnirman, *J. Low Temp. Phys* **118**, 751 (2000).
- [43] M. A. Nielsen and I. L. Chuang, *Quantum Computation and Quantum Information* (Cambridge University Press, 2000).
- [44] M. J. Lea, P. G. Frayne, and Yu. Mukharsky, *Fortschr. Phys* **48**, 1109 (2000).
- [45] W. K. Wootters, *Phys. Rev. Lett.* **80**, 2445 (1998).

- [46] G. Burkard, D. Loss, D. P. DiVincenzo, and J. A. Smolin, *Phys. Rev. B* **60**, 11404 (1999).
- [47] D. P. Divincenzo, G. Burkard, D. Loss, and E. V. Sukhorukov, in *Quantum Mesoscopic Phenomena and Mesoscopic Devices in Microelectronics*, edited by I. O. Kulik and R. Ellialtioglu (1999), cond-mat/9911245.
- [48] A. V. Khaetskii and Y. V. Nazarov, *Phys. Rev. Lett.* **61**, 12639 (2000).
- [49] S. Debald, T. Brandes, and B. Kramer, *Phys. Rev. B* **66**, 041301(R) (2002).
- [50] C. S. Lent, M. Liberman, and G. L. Snider, in *Proceedings of Molecular Electronics 2000* (2000).
- [51] D. P. DiVincenzo, *J. Appl. Phys.* **85**, 4785 (1999).
- [52] This is in fact an approximation since the Schrödinger equation is not strictly separable and integration over the lowest bound-state in the z-direction modifies the Coulomb interaction. However, the error due to this approximation is small and unimportant for what follows.
- [53] In fact  $\Phi = BA$ , where  $A$  is an effective area of the dot which is slightly smaller than its actual area, reflecting the fact that the charge density peaks for the electrons are not precisely in the corners of the dot.
- [54] In fact the role of singlets and triplets reverse for half flux quantum through the dot. It is straightforward to show that the electrons have the same behaviour as fictitious hard core spin-bosons. The ‘particles’ may be regarded as ‘composite fermions’ for this two-electron system.

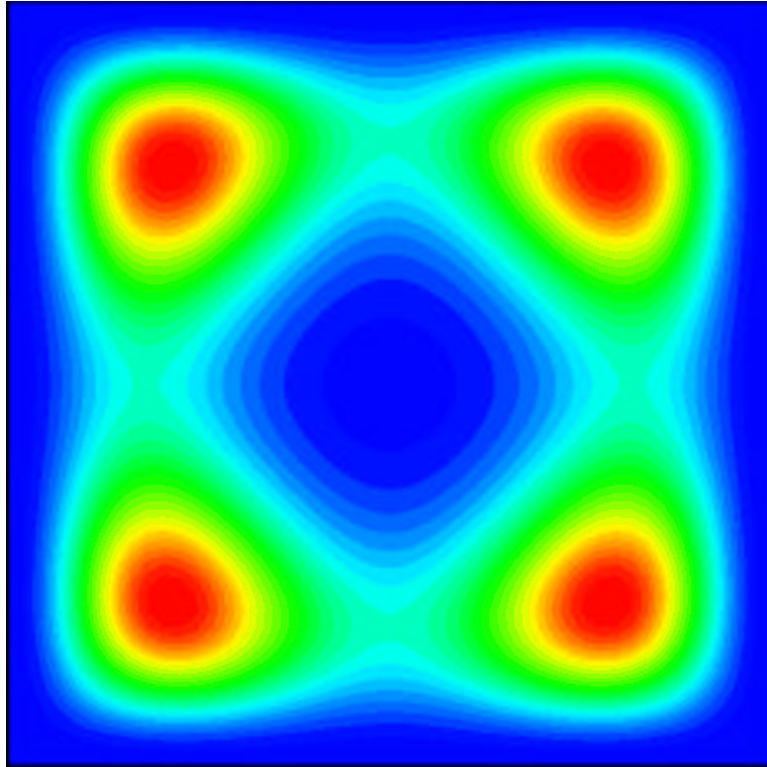


FIG. 1: Ground-state charge density, peaked in diagonally-opposite corners, for a two-electron GaAs quantum dot with side length 800nm ( $\approx 100$  effective Bohr radii).

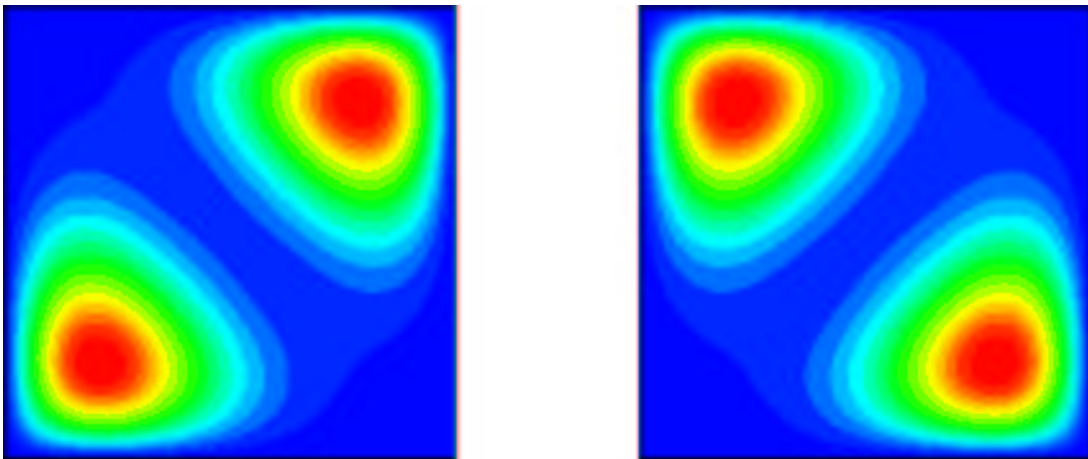


FIG. 2: Contour plots of two-electron basis functions which yield the ground-state charge density of figure 1.



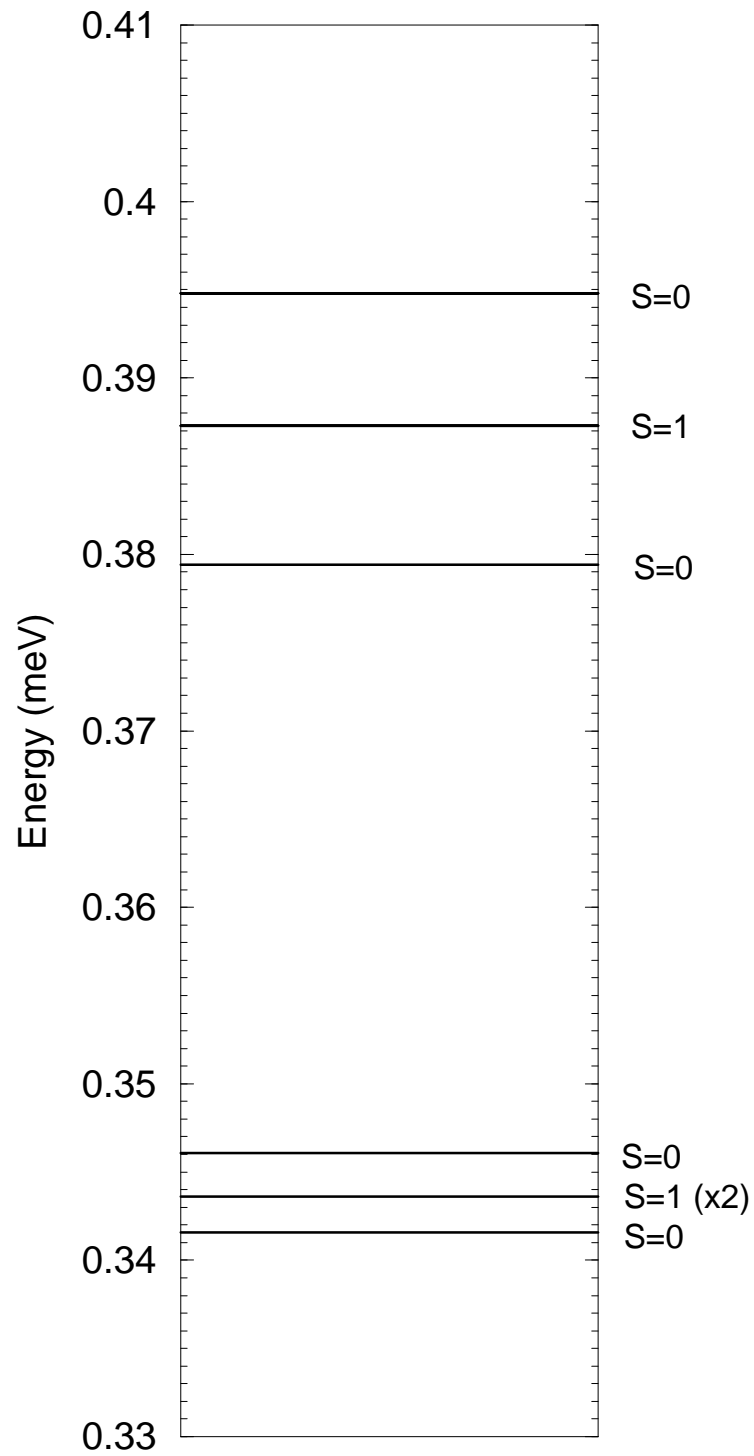


FIG. 3: Energy spectrum of a two-electron quantum dot showing an isolated low-lying manifold of two singlets and two triplets.

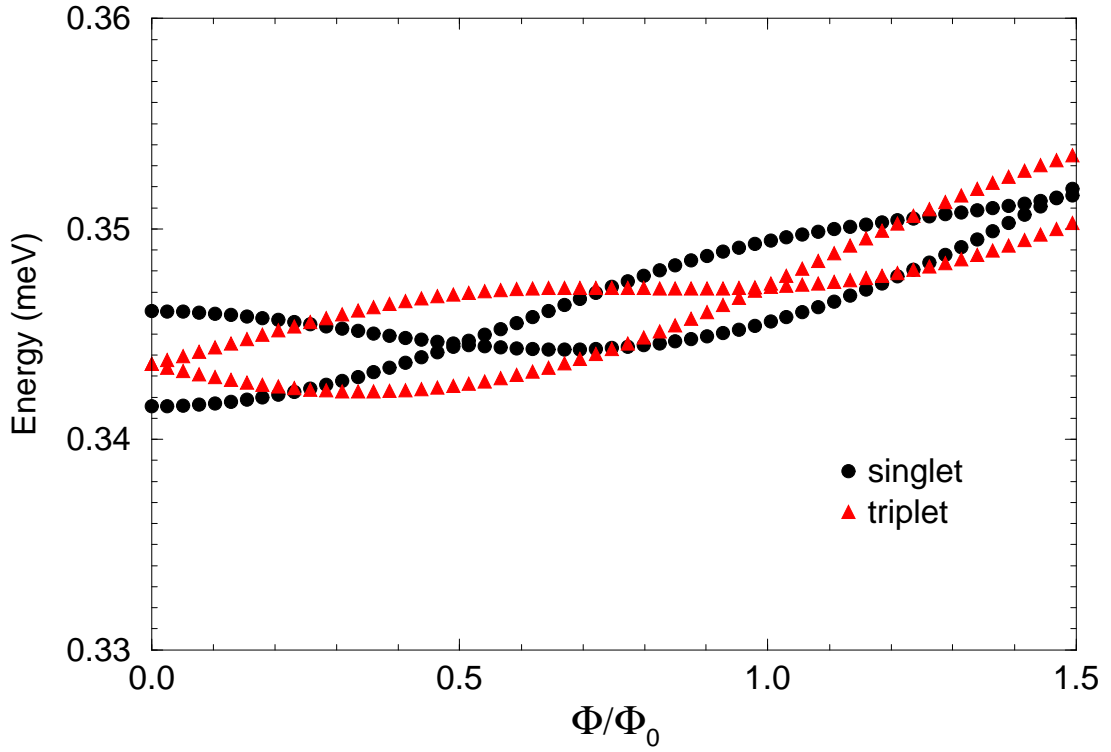


FIG. 4: Variation of low-lying eigenenergies with magnetic flux of a two-electron quantum dot.  $\Phi_0 = h/e$  is the flux quantum.

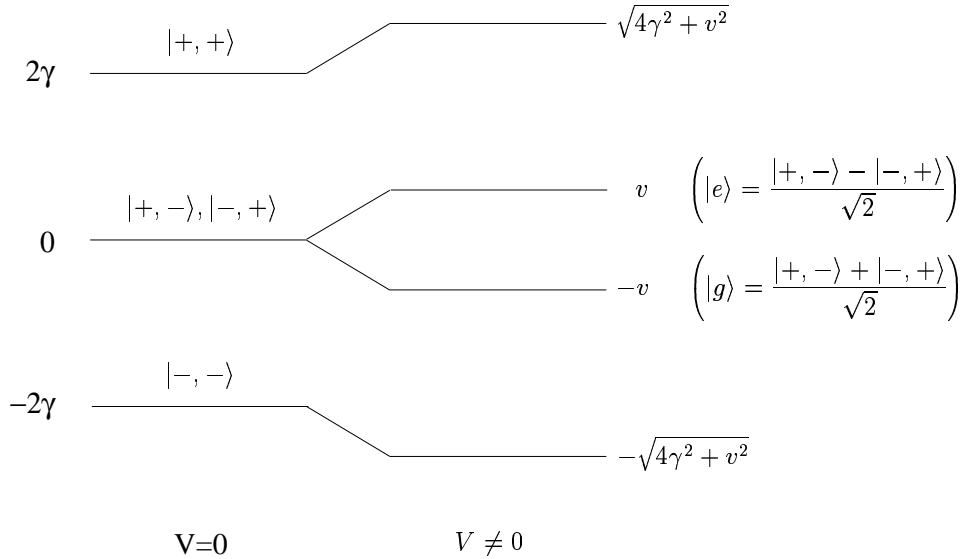


FIG. 5: Eigensolutions of the two-qubit quantum-dot Hamiltonian with weak coulomb repulsion between cells.

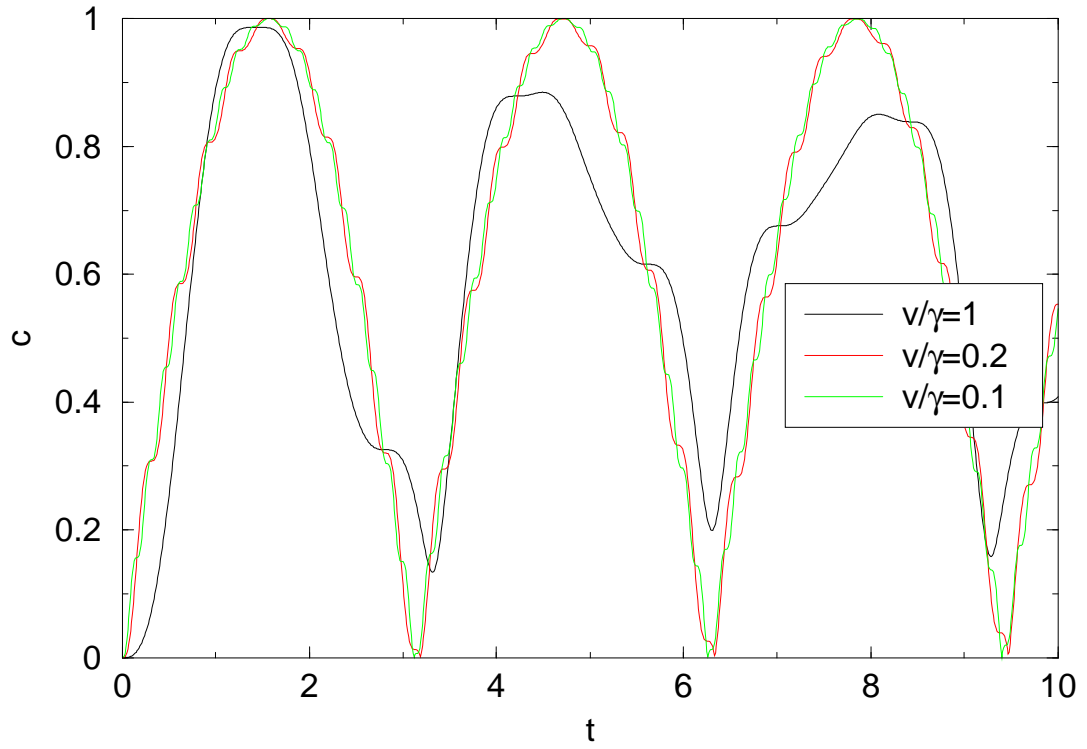


FIG. 6: Concurrence for starting state  $|0,0\rangle$  and  $v/\gamma = 1, 0.2$  and  $0.1$ , showing oscillations on a timescale  $\hbar/\gamma$  before reaching full entanglement.

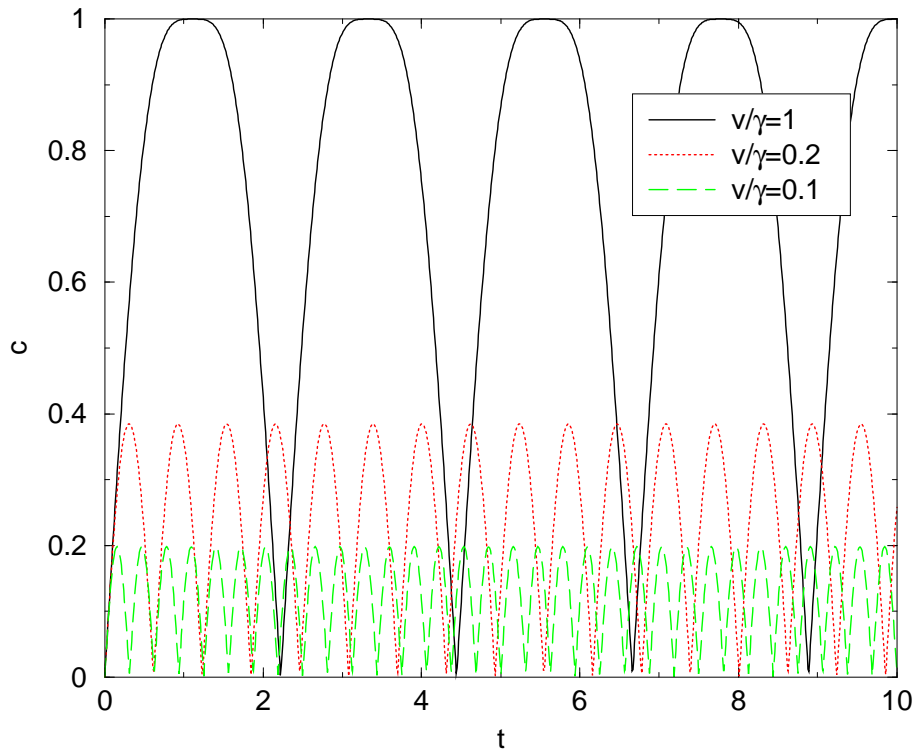


FIG. 7: Time dependence of concurrence for an initial state  $|+, -\rangle$  in which  $\gamma = 0$  on one dot.

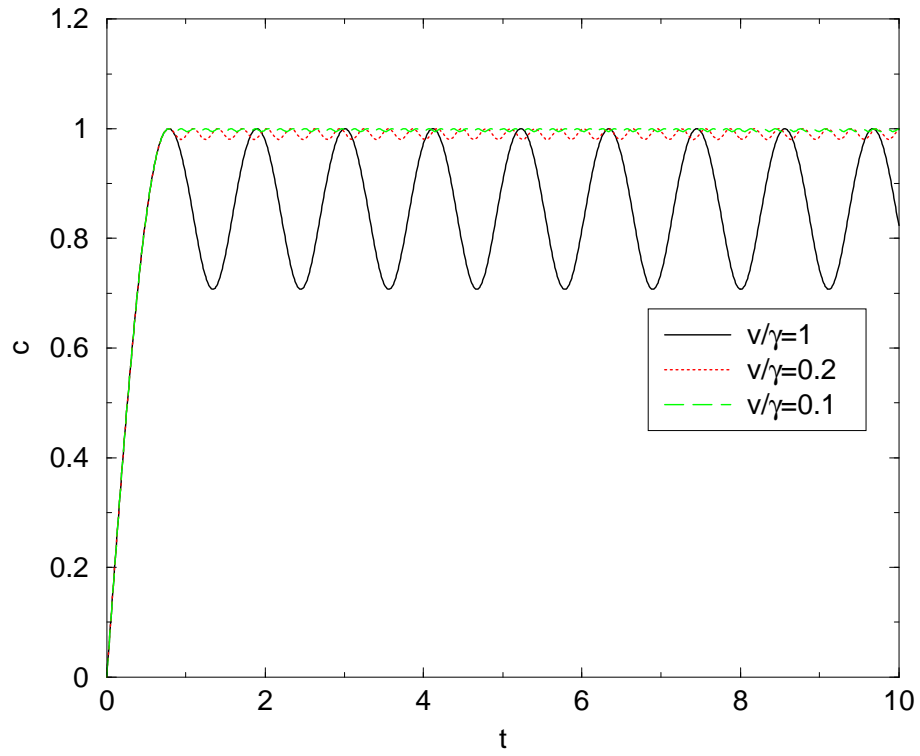


FIG. 8: Time dependence of concurrence with an initial state  $|+, -\rangle$  for which  $\gamma$  is switched off on one dot only at  $t = \pi/4v$ .

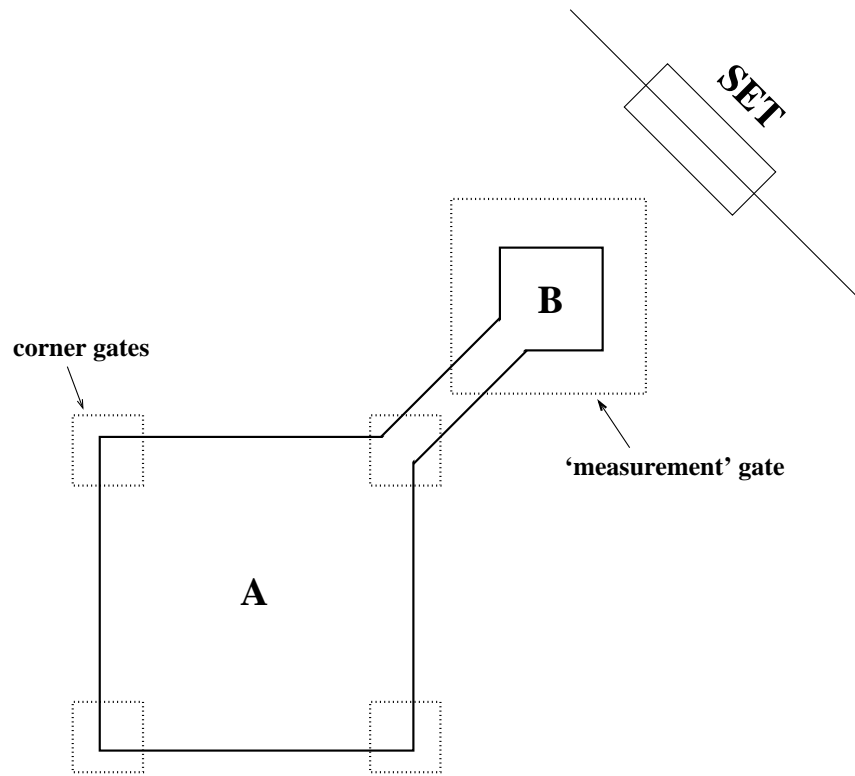


FIG. 9: Schematic diagram showing arrangement for final-state measurement.